THE ASTROPHYSICAL JOURNAL, 278:619–629, 1984 March 15

NEAR-INFRARED SPECTROPHOTOMETRY OF CRAB NEBULA FILAMENTS

RICHARD B. C. HENRY[1]
Physics Department, University of Delaware; and Department of Astronomy, University of Michigan
AND
GORDON M. MACALPINE[1] AND ROBERT P. KIRSHNER[1,2]
Department of Astronomy, University of Michigan
Received 1983 June 15; accepted 1983 August 22

ABSTRACT

Spectra from roughly 6500 Å to 10200 Å of 14 positions in the Crab nebula have been obtained using the Cryogenic Camera and the KPNO 4 m telescope. This spectral region includes lines of [S II], He I, [Ar III], [O II], [Ni II], [Fe II], [S III], [C I], and He II. Relatively strong [C I] λλ9823, 9850, [Ni II] λ7378, and [Fe II] λ8617 emission was observed in nearly all filaments. Some of the strength of the carbon lines might be explained by allowing for collisional excitation by neutral atomic hydrogen. Data for seven filaments were linked to available optical observations of the same positions to search for correlations between various lines and to derive [O II] temperatures. A direct correlation between [O III] λ5007/[O II] λ3727 and [S III] λ9532/[S II] λ6724 was found, suggesting that the latter is a good ionizing flux diagnostic. The abundance of nickel may exceed the cosmic level by at least an order of magnitude, while the abundance of iron appears to be somewhat lower than normal. One interpretation of this result is that iron is incorporated into grains more readily than nickel.

Subject headings: nebulae: abundances — nebulae: Crab Nebula — nebulae: supernova remnants — spectrophotometry

I. INTRODUCTION

The filaments of the Crab nebula are the debris from a recent (A.D. 1054) supernova event which took place about 200 pc below the galactic plane and are believed to be relatively undiluted by interstellar matter. A careful analysis of the emission lines from the filaments should, therefore, provide information about the mass and evolution of the precursor star, as well as the physical details of the explosion itself. Recently a number of spectrophotometric studies of the filaments have been carried out using linear detectors which provide a qualitative improvement over the pioneering work by Woltjer (1958), using spectra taken by N. U. Mayall. The recent investigations by Davidson (1978, 1979), Miller (1978), and Fesen and Kirshner (1982) provide high-quality spectra in the optical range for numerous positions. In addition, data for Miller's (1978) position 2 have now been extended into the UV by Davidson *et al.* (1982) and into the near-infrared by Dennefeld and Péquignot (1982).

Analyses of the available data have been carried out by Henry and MacAlpine (1982) and Péquignot and Dennefeld (1983) using detailed photoionization modeling techniques. These two studies suggest that: (1) the relative abundance of helium is high in many filaments and may vary among positions observed; (2) the precursor star most likely had a mass greater than 3 $M_\odot$; and (3) the individual filaments are surrounded by zones of high ionization, probably as a result of the gas being ionized by an enveloping source rather than the distant (plane-parallel) source assumed for simplicity in the models.

[1] Visiting Astronomer, Kitt Peak National Observatory, operated by the Association of Universities for Research in Astronomy, Inc., under contract with the National Science Foundation.
[2] Alfred P. Sloan Foundation Research Fellow.

Due to past instrumental limitations, most of our information for comparison to models has come from optical data covering the 3700–7000 Å spectral range. UV and near-infrared data are only available for Miller's position 2. Yet, as Péquignot and Dennefeld have demonstrated, important physical and chemical information can be gained by extending the observations of more filaments into the near infrared. The spectral region between 7000 and 10000 Å contains lines of He I, [O II], [Ar III], [Ni II], [Fe II], [S III], and [C I]. Information about gas temperature and ionizing flux can be derived by combining strengths of [O II] λ7325 and [S III] λλ9069, 9532, respectively, with existing optical data; and lines of [Ni II] λ7378 and [C I] λλ9823, 9850 may supply important abundance or optical depth information. In addition, it is especially desirable to have spectra of many positions throughout the filamentary system to check on inhomogeneities and to establish correlations between various chemical and physical parameters.

In this paper we report observations of 14 positions in the Crab filaments from roughly 6500 Å to 10200 Å, using the Cryogenic Camera and the KPNO 4 m telescope. Nine of these positions have previously been observed in the optical portion of the spectrum, and the spectra for seven of them can be linked to provide coverage from 3700 Å to 10000 Å. In § II we describe the observations, and in § III we present a discussion of the results. Section IV is a summary of our findings.

II. OBSERVATIONS

a) Data Aquisition

Simultaneous spectra of 14 positions were obtained on each of the nights of 1981 December 20 and 21, using a multi-aperture plate with the Ritchey-Chrétien spectrograph and Cryogenic Camera attached to the KPNO 4 m telescope. The

spectral coverage of roughly 6500–10200 Å was obtained by employing two transmission grating prisms with nominal ranges of 6500–9500 Å and 8200–11000 Å, along with order separating filters. The effective red limit was 10200 Å because of the rapid drop in response of the CCD chip longward of 9800 Å.

A multi-aperture plate, in which holes had been drilled at precisely measured locations, was placed in the focal plane of the spectrograph. Light from each aperture was subsequently dispersed and focused on an 800 × 800 pixel Texas Instruments CCD detector. Each aperture plate hole measured 4″ in diameter on the sky, which, when combined with either transmission grating prism, gave a spectral resolution estimated to be 25 Å with a dispersion of about 4.05 Å per pixel. The spatial resolution perpendicular to the dispersion was 0.″65 per pixel. Details of the observations are summarized in Table 1. Sky integrations were made following the object integrations and were, therefore, not simultaneous. The two-dimensional digital data were subsequently reduced to one-dimensional IIDS-formatted spectra at KPNO, and then further reduced to flux vs wavelength using reduction routines available at the University of Michigan. We shall discuss the details of the reduction procedure below.

Precise telescope positioning was accomplished by drilling in the aperture plate two "setup" holes which aligned with field stars. Once correct positioning was obtained, the telescope was offset by a predetermined distance so that the object holes aligned with the filament positions to be observed, and the setup stars were occulted.

Most of our selected positions in the Crab were chosen to coincide with those observed in the visible by Fesen and Kirshner (1982) (their positions 1, 3, 5, 6, 7, 8, 9, 10). These are shown in Figure 1 of their paper and will be designated FK1, FK3, . . . , etc. here. In addition, data were obtained for Miller's (1978) position 2 (M2) and two locations never observed previously (HMK1 and HMK2). The positions corresponding with the two setup holes after offsetting the telescope, plus a sky hole originally intended for sky subtraction also showed emission (although definite filamentary structure is absent) and are designated as HMK3, HMK4, and HMK5, respectively. The locations of HMK1, HMK2, HMK3, HMK4, and HMK5 are illustrated in Figure 1. In Table 2 we have listed the locations of all observed positions relative to star 16 in Wyckoff and Murray (1977).

b) *Reduction Procedure*

Prior to reduction, the data were in the form of frames of size 512 × 800 pixels, each containing 14 spectra. For each night we obtained several object and sky frames plus a quartz continuum lamp frame. The initial data reductions were carried out at KPNO where, after converting each frame to IPPS format, dark subtractions were performed by determining an average dark count from unexposed areas of each raster and subtracting this amount from each pixel of the same raster. Henceforth, the procedural summary pertains to one night's data.

The quartz continuum lamp frame was used to generate a polynomial model describing the position, intensity, and width of each of the 14 individual spectra. This model was then divided by the quartz raster itself to produce a normalized quartz frame for flat fielding. The object and sky rasters were then corrected for any vertical shift due to instrument flexure (by correlating them with the quartz raster) and flat fielded with the normalized quartz frame to remove small-scale detector sensitivity variations. Using the polynomial model, individual spectra were then extracted from all of the frames, producing an object and sky spectrum in IIDS format (i.e., counts versus channel) for each of the 14 aperture positions of each frame.

The final reductions of these one-dimensional spectra were carried out at the University of Michigan using standard spectrophotometric reduction methods. The numerous bright sky lines present throughout the observed spectral range were used to calibrate the wavelength scale for each scan. In order to minimize the effects of possible dispersion variations over the CCD chip, each spectrum from the sky frame was used to calibrate the filament spectrum observed with the same aperture on the same night. Data for the night sky lines were taken from Broadfoot and Kendall (1968) and Bass and Garvin (1962). Object and sky integrations were not simultaneous, and noticeable variations in the relative strengths of the sky lines produced by different molecules were present among the frames, making good sky subtraction difficult. To obtain a sky-subtracted object scan, each sky spectrum was multiplied by a range of constants and subtracted from its paired object spectrum. The smoothest of the resulting scans was then corrected for atmospheric extinction and fluxed, using long-slit spectra of well-known standards observed on the same night.

TABLE 1

OBSERVING LOG

UT Date	Sky Conditions	Total Integration Time (s)	Spectral Range (Å)	Sky Field Center (arc min)
1981 Dec 20.....	Clear	6000	6500–9500	30.7 S
1981 Dec 21.....	Clear	4000	8200–11000	30.0 N

TABLE 2

APERTURE LOCATIONS[a]

Position Name	ΔX	ΔY
FK1.....	64.″8 E	2.″0 S
FK3.....	36.9 E	68.9 N
FK5.....	8.9 E	59.5 N
FK6.....	4.9 E	78.2 N
FK7.....	33.7 W	39.5 N
FK8.....	96.0 W	68.5 N
FK9.....	69.7 W	24.3 S
FK10.....	29.6 E	60.4 S
M2.....	39.6 W	18.6 S
HMK1.....	11.4 W	29.6 S
HMK2.....	28.4 W	84.2 S
HMK3.....	27.8 E	101.8 S
HMK4.....	27.9 W	101.8 N
HMK5.....	65.4 E	122.0 S

[a] Epoch 1982.0 offsets (±0.″5) given with respect to star 16 in Wyckoff and Murray 1977, where $\alpha = 5^h31^m31^s.6$ and $\delta = +21°58'58''$ for epoch 1950.0.

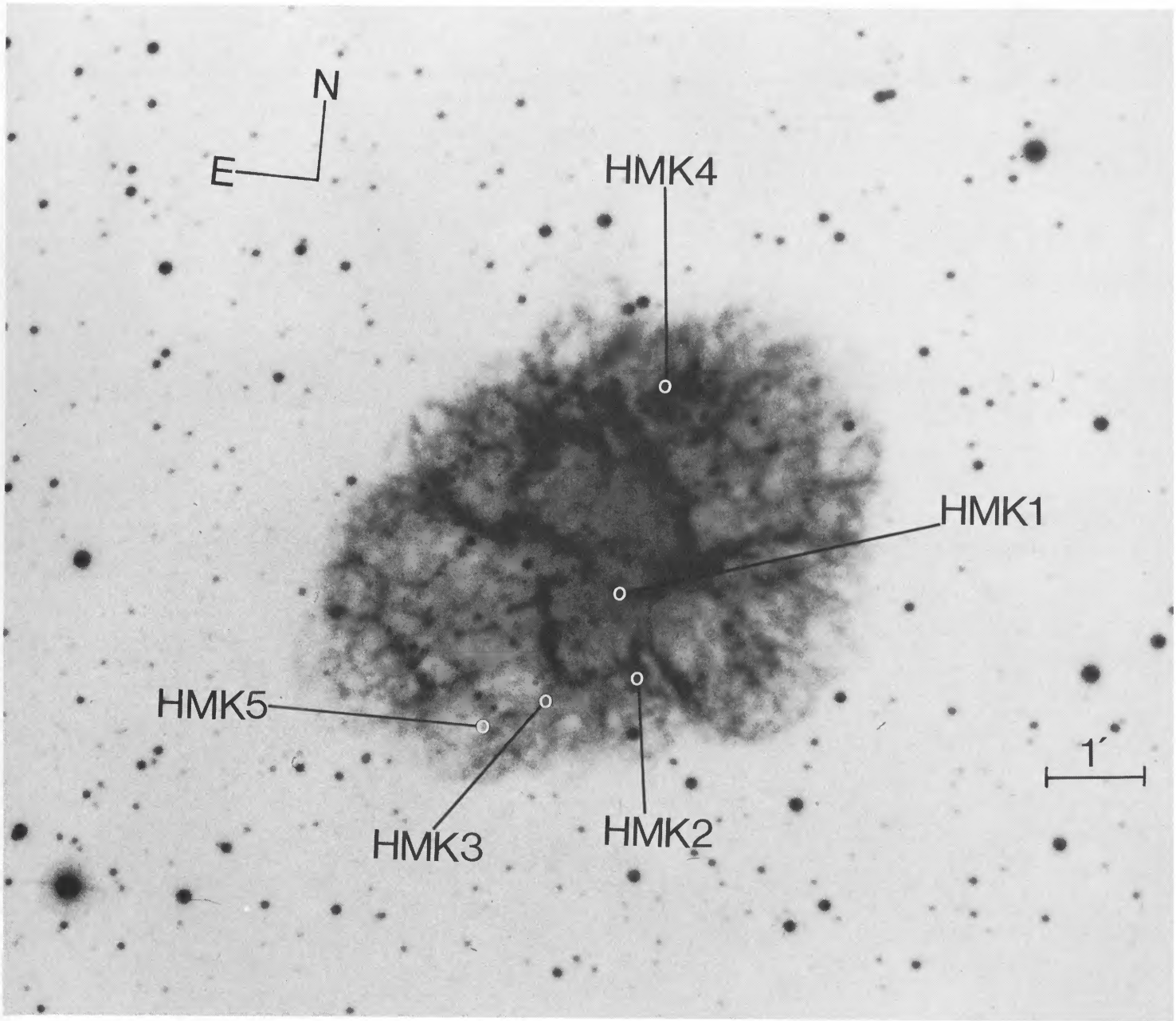

FIG. 1.—Narrow-band interference filter photograph of the Crab nebula in Hα, obtained by S. R. Schurmann in 1981 at McGraw-Hill Observatory with a 144 mm image tube, showing the locations of those positions discussed in this paper which have not been reported upon in previous papers.

TABLE 3

RELATIVE EMISSION-LINE INTENSITIES
($I_{[S\,II]} = 100$; $E_{B-V} = 0.5$)

		FILAMENT POSITIONS													
		FK1		FK3[a]		FK5		FK6		FK7		FK8		FK9	
LINE ID	λ(Å)	$F(\lambda)$	$I(\lambda)$	$F(\lambda)$	$I(\lambda)$	$F(\lambda)$	$I(\lambda)$	$F(\lambda)$	$I(\lambda)$	$F(\lambda)$	$I(\lambda)$	$F(\lambda)$	$I(\lambda)$	$F(\lambda)$	$I(\lambda)$
Hα + [N II]	6563, 6548, 6584	...	...	...	...	...	...	...	...	...	...	113	116	294	300
He I	6678	...	...	...	...	...	...	...	...	...	...	...	...	(9)	(9)
[S II]	6716, 6731	100	100	...	...	100	100	100	100	100	100	100	100	100	100
He I	7065	(2)	(2)	100	100	(2)	(2)	(1)	(1)	1	1	3	2	4	4
[Ar III]	7136	15	14	600	594	11	11	9	8	11	10	9	8	8	7
[O II]	7325	8	7	720	691	8	7	(6)	(5)	9	8	13	11	21	19
[Ni II]	7378	7	6	2000	1900	16	14	29	26	12	11	23	21	8	7
[Ar III]	7751	5	4	(210)	(187)	(3)	(2)	(2)	(2)	2	1	...	...	...	...
[Fe II]	8617	(1)	(1)	1100	836	12	9	7	5	4	3	6	4	8	6
P 13	8665	...	...	350	266	...	...	(2)	(1)	...	...	(1)	(1)	5	4
[S III]	9069	45	30	1800	1278	24	16	17	12	35	24	26	17	21	14
[S III]	9532	88	55	4900	3185	44	27	36	22	78	49	44	28	41	26
[C I]	9823, 9850	19	11	1800	1116	7	4	7	4	16	10	37	22	68	40
He II	10123	12	7	...	...	...	...	...	...	...	...	3	1	2	1
f([S II] λλ6716, 6731) ergs cm^{-2} s^{-1}		1.1 E-13		...		1.4 E-13		2.3 E-13		7.9 E-14		1.6 E-13		6.8 E-14	
I([S II] λλ6716, 6731)/I(Hβ)[b]		3.14		...		4.28		5.58		4.35		5.58		...	

		FILAMENT POSITIONS													
		FK10		M2		HMK1		HMK2		HMK3		HMK4		HMK5	
LINE ID	λ(Å)	$F(\lambda)$	$I(\lambda)$	$F(\lambda)$	$I(\lambda)$	$F(\lambda)$	$I(\lambda)$	$F(\lambda)$	$I(\lambda)$	$F(\lambda)$	$I(\lambda)$	$F(\lambda)$	$I(\lambda)$	$F(\lambda)$	$I(\lambda)$
Hα + [N II]	6563, 6548, 6584	89	91	163	167	117	120	86	88	22	23	...	...	67	68
He I	6678	...	...	4	4	(5)	(5)	2	2	11	11	...	...	...	...
[S II]	6716, 6731	100	100	100	100	100	100	100	100	100	100	100	100	100	100
He I	7065	(2)	(2)	5	5	(3)	(3)	(1)	(1)	3	2	2	2	...	...
[Ar III]	7136	8	8	(8)	(7)	(8)	(7)	(9)	(9)	16	15	14	13	4	4
[O II]	7325	7	6	24	22	7	6	5	5	8	7	8	8	...	...
[Ni II]	7378	10	9	11	10	8	7	5	5	42	38	23	21	11	10
[Ar III]	7751	(2)	(1)	5	4	...	...	2	2	...	...	...	...	...	...
[Fe II]	8617	(3)	(2)	3	2	...	...	2	1	26	19	10	7	...	...
P 13	8665	...	...	...	...	...	...	...	...	...	...	...	...	...	...
[S III]	9069	16	11	46	31	19	13	21	14	27	18	21	14	...	...
[S III]	9532	31	19	88	54	40	25	44	27	65	41	36	22	...	...
[C I]	9823, 9850	16	10	40	24	14	8	9	5	18	11	5	3	...	...
He II	10123	(1)	(1)	8	5	(2)	(1)	...	...	...	...	...	...	...	...
f([S II] λλ6716, 6731) ergs cm^{-2} s^{-1}		3.6 E-13		1.6 E-13		1.2 E-13		1.4 E-13		2.6 E-14		1.2 E-13		1.8 E-13	
I([S II] λλ6716, 6731)/I(Hβ)[b]		12.51		(3.51)[c]		...		...		...		...		...	

[a] I(He I λ7065) = 100.
[b] From Fesen and Kirshner 1982.
[c] From Davidson *et al.* 1982.

c) *Line Strengths*

Measured line strengths are given by position in Table 3. For each filament location, we have listed the observed and dereddened flux ratios, F and I, respectively, normalized to the [S II] λ6724 blend, along with the measured absolute fluxes of the [S II] blend, uncorrected for interstellar extinction. Corrections for interstellar reddening were performed by employing the reddening curve from Osterbrock (1974) and assuming that $E_{B-V} = 0.5$, as determined by Miller (1973) and Wu (1981). For those positions where there are two velocity components, we report line strengths only for the brighter one. For those positions at which we *and* Fesen and Kirshner (1982) (FK1–FK10) or Davidson *et al.* (1982) (M2) measured [S II] $\lambda\lambda$6716, 6731, Table 3 also contains [S II] $\lambda\lambda$6716, 6731/Hβ ratios.

The accuracy of our measured line strengths is influenced by three factors: (1) residual sky emission after sky subtraction, (2) accuracy of the response curve, and (3) photon statistics. We estimate an overall error in the relative strengths given in Table 3 of 15%–20% for the lines of Hα + [N II], [S II], and [S III] and 20%–30% for most other features. Blended features, which were measured by fitting a Gaussian profile to each component, may be less accurate. In Table 3, line strengths with uncertainties estimated to be greater than 50% are enclosed in parentheses.

III. DISCUSSION

Figures 2 and 3 contain plots of the two spectral regions observed for each position. (Data for HMK5 in the $\lambda\lambda$8200–10200 spectral range are not shown, since the signal-to-noise ratio was very low for this faint position.) We have also included a sky scan with each set of plots in order to assist the reader in distinguishing between object and sky lines where sky subtraction is incomplete. Figure 4 shows enlarged plots for FK10 with all of the lines in Table 3 identified.

An interesting feature in a number of the spectra is the strong [Fe II] λ8617 line, seen also by Dennefeld and Péquignot (1982) in M2. The fact that it is real and not simply the result of poor subtraction of the coincident atmospheric O_2 bands is supported by the presence, at position FK3, of two velocity components of the λ8617 line which match those of other lines. In addition, lines of the same multiplet (13F), λ9227 and λ9399, are generally present in spectra with strong λ8617. In several filaments we also observe a feature on the red wing of [Ar III] λ7135, which is probably [Fe II] λ7155.

Lines of [Fe II], [Fe III], [Fe V], and [Fe VII] were observed by Fesen, Kirshner, and Chevalier (1978) and Fesen and Kirshner (1982), but, to our knowledge, no forbidden iron line has been found to be as strong as the [Fe II] λ8617 feature. This line corresponds to an $a^4F_{9/2}$–$a^4P_{5/2}$ transition and must be produced collisionally, since recombination or resonance fluorescence would also produce strong permitted lines (see Phillips 1978). Furthermore, data in Nussbaumer and Storey (1980) show that the upper level must be excited almost exclusively from the ground $a^6D_{9/2}$ level of Fe^+. Excitation of the line by first populating $^4F_{9/2}$ through charge exchange (Dalgarno and Butler 1978) and subsequently exciting the electron collisionally to the $^4P_{5/2}$ level can be ruled out, since, according to Nussbaumer and Storey, spontaneous decay of $^4F_{9/2}$ is favored by five orders of magnitude over collisional excitation to the ^4P term. The ^4P term is the lowest lying one which can decay and emit a photon in the visible or near-infrared. Since λ8617 is also more highly favored than all other transitions from the ^4P term (see Nussbaumer and Storey 1980), one would expect it to be the strongest [Fe II] feature present in visible or near-infrared data, as we have observed it to be.

Fe^+ should be the primary ionization stage of iron in the portion of the filament dominated by H^0 because of the low ionization potential of Fe^0. We might, therefore, expect the strength of [Fe II] to be correlated with that of [S II] throughout the nebula, since most sulfur is in the S^+ stage in the H^0 zone (see Henry and MacAlpine 1982). In Table 4, where we show a number of correlation coefficients for various line ratios and pairs, it can be seen that [Fe II] and [S II] are reasonably correlated.

Our average observed flux ratio of [S III] λ9532/λ9069 is 1.94 ($\sigma = 0.25$) for 13 filaments, which is close to the value of 1.78 observed by Dennefeld and Péquignot (1982) for M2. (Our value for M2 is 1.77.) Since the two relevant transitions have the same upper level, the intensity ratio is independent of physical parameters in the gas and is predicted to be 2.43, using transition probabilities from Garstang (1968). Near-infrared observations of the Orion nebula by Foukal (1974) and Aller and Liller (1959), NGC 2440 by Condal (1982), and NGC 7027 by Condal *et al.* (1981) indicated no atmospheric effects on the measured [S III] line ratio. However, Dennefeld and Péquignot conclude that their measured value of $I(\lambda9532)/I(\lambda9069)$ is low due to greater atmospheric absorption of λ9532 emission by an H_2O band, a conclusion which appears to be consistent with the results of Dennefeld and Stasińska (1983). Another plausible explanation is that either atmospheric absorption or emission caused the instrumental response curve to be lower or higher, respectively, over the bandpasses containing λ9069 or λ9532. This would alter their ratio in the observed sense.

Table 4 shows the measured [O III] λ5007/[O II] λ3727 (from Fesen and Kirshner 1982 or Davidson *et al.* 1982) and our [S III] λ9532/[S II] $\lambda\lambda$6716, 6731 ratios to be directly correlated among the filaments. However, the photoionization models by Henry and MacAlpine (1982) predicted that these ratios should be *inversely* correlated. The filament-to-filament variations in the calculations result from differences in adopted impingent ionizing radiation fluxes. The [O III] emission arises within the H^+ domain, [O II] and [S III] emission arises near and within the $H^+ \rightarrow H^0$ transition zone, and [S II] comes primarily from the H^0 region. A higher incident ionizing flux increases the size of the H^+ domain relative to the

TABLE 4

EMISSION-LINE CORRELATIONS

Line Pairs Tested	Correlation Coefficient	Confidence Level[a]
[S III]/[S II]:[O III]/[O II]	0.72[b]	>0.90
[Fe II]:[S II]	0.65[b]	<0.90
[C I]:[S II]	0.22[b]	...
[Ni II]:[S II]	0.95[b]	>0.99
[C I]:[Ni II]	0.56	>0.90

[a] 1.0 minus the confidence level is the probability of a similar value for the correlation coefficient occurring for an uncorrelated sample.

[b] FK10 not included because of unusually strong [S II].

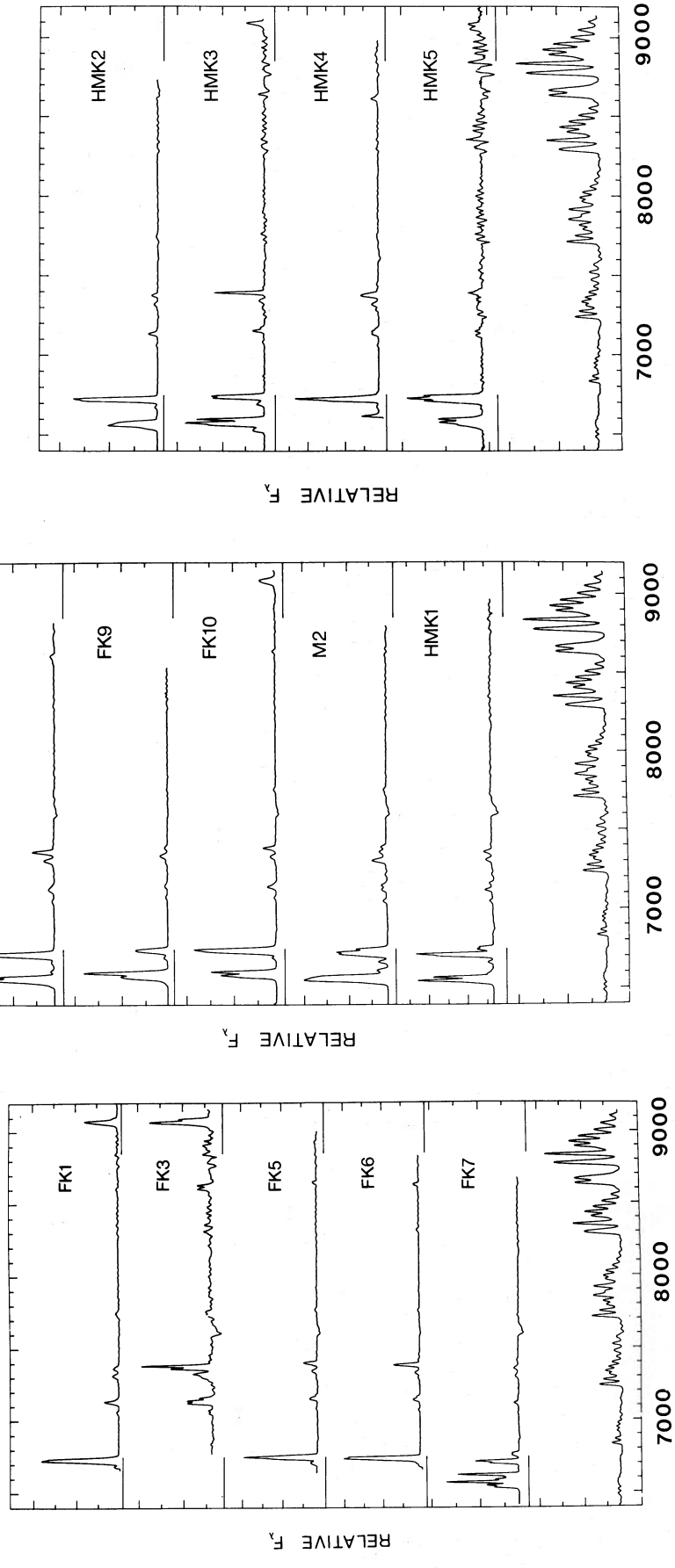

FIG. 2.—Spectrophotometric scans of 14 filament positions in the Crab nebula between 6500 and 9200 Å. Relative flux density is plotted as a function of wavelength in angstroms. A sky scan is included at the bottom of each figure to assist in identifying sky features in those cases where sky subtraction was incomplete.

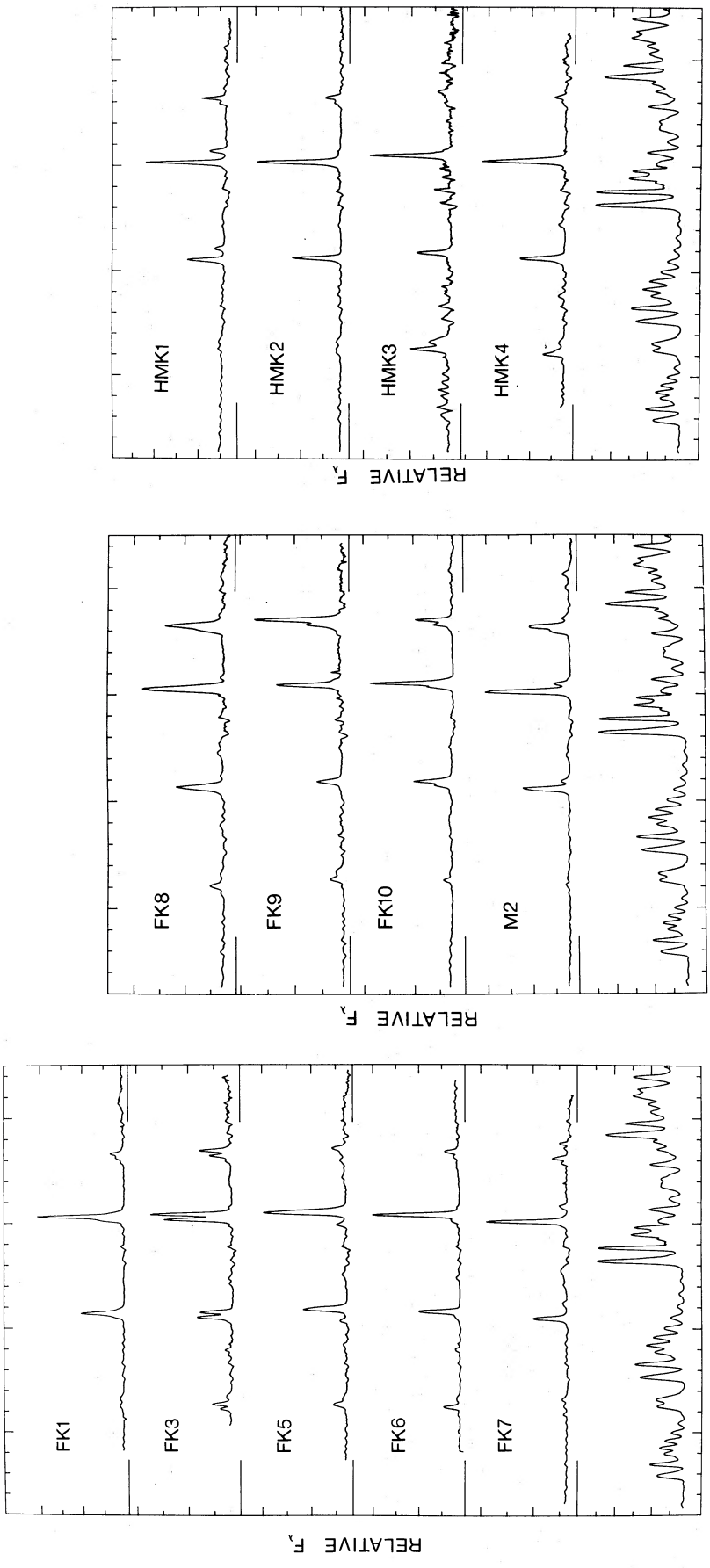

FIG. 3.—Spectrophotometric scans of 13 filament positions in the Crab Nebula between 8200 and 10200 Å. Relative flux density is plotted as a function of wavelength in angstroms. A sky scan is included at the bottom of each figure to assist in identifying sky features in those cases where sky subtraction was incomplete.

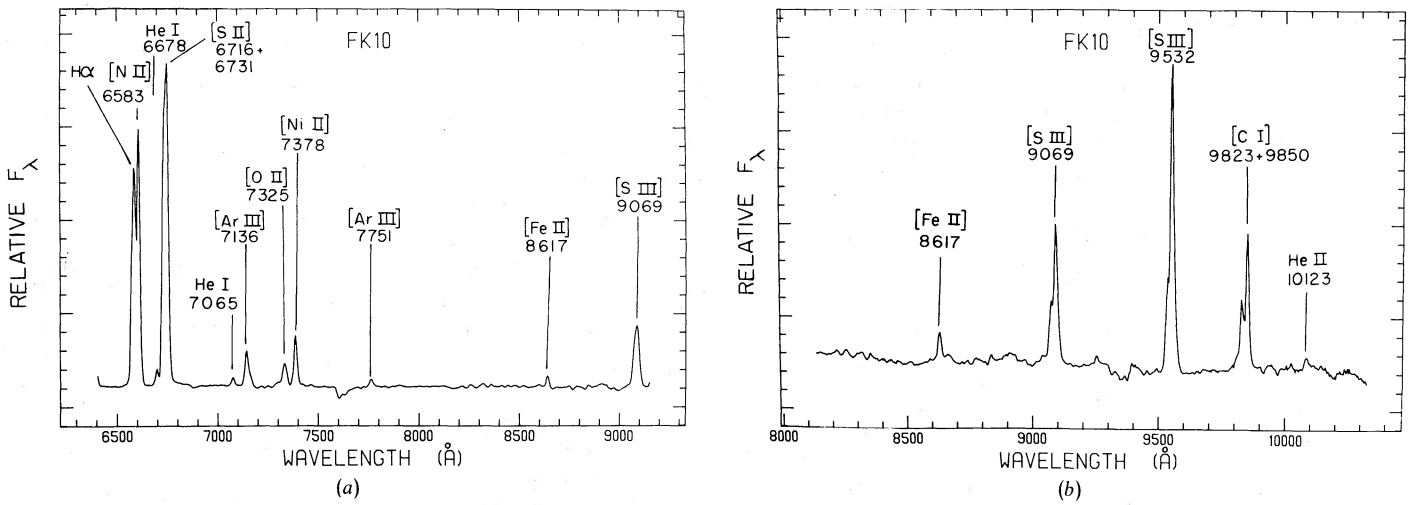

FIG. 4.—Enlarged scans of FK10 identifying the lines listed in Table 3 and discussed in the text. Note the presence of a weaker velocity component which is slightly blueshifted with respect to the stronger one and is most conspicuous for lines which are redward of 9000 Å.

$H^+ \rightarrow H^0$ transition region (Feldman 1979), thereby increasing calculated [O III]/[O II] line ratios. On the other hand, by increasing the size of the $H^+ \rightarrow H^0$ transition region relative to the rest of the filament, the increased flux could be expected to lead to lower calculated [S III]/[S II] ratios. In addition, adapting equation (10) from MacAlpine (1972) to the presently adopted plane-parallel geometry, we have

$$F_\nu[R(H^+)] \propto F_\nu \exp\left[-\kappa_\nu F_\nu\right], \quad (1)$$

which says the flux of medium-high frequency photons reaching the Strömgren edge, $[R(H^+)]$, is proportional to the input flux, F_ν, attenuated by an optical depth $\kappa_\nu F_\nu$. This expression for optical depth uses the fact that the Strömgren thickness is proportional to F_ν. From expression (1), we see that, under the right conditions, lowering F_ν can actually result in increased S^{+2}/S^+ ionization at the Strömgren edge and beyond, thereby contributing to the calculated correlation. However, a decrease in the adopted model pressure would lower the κ_ν term in expression (1), and this could cause $F_\nu[R(H^+)]$ to correlate directly with F_ν, thereby reversing the effect cited above and leading to a direct correlation between calculated [S III]/[S II] and [O III]/[O II] line ratios, in agreement with the observations. Of course, the pressure in the models cannot be lowered very much, as the agreement between calculated and observed [S II] $\lambda\lambda$6731/6716 ratios would be less satisfactory.

Further examination of the correlation coefficients in Table 4 reveals that the observed strengths of [Ni II] and [S II] are directly related, as one would expect from ionization potential considerations. These lines originate largely from the H^0 zone. However, the absence of any strong correlation between [C I] and [S II] is intriguing. If we assume that the gas is optically thin to photons with energy less than 13.6 eV, then the relative abundances of C^0 and C^+ should remain roughly constant in the H^0 zone, and the [C I] line strengths should correlate directly with [S II] emission. Indeed, recent observations of [C I] in NGC 6720 by Jewitt *et al.* (1983) seem to give observational support to this contention. The lack of a strong correlation in our data for the Crab suggests that additional factors may be influencing [C I] emission.

The observed strength of [C I] $\lambda\lambda$9823, 9850 in our data is greater than that predicted by the photoionization models of Henry and MacAlpine (1982) for both FK5 and FK8, the two positions modeled in that paper. For FK5, the calculated strength is smaller by a factor of 3, while, for FK8, it is smaller by an order of magnitude. Strong [C I] emission in the Crab was originally reported for one filament by Dennefeld and Andrillat (1981). In an effort to match that observation, Henry and MacAlpine attempted to increase the strength of [C I] by raising the relative abundance of carbon. However, the resulting [O III] temperatures were much lower than those derived from observations because of the importance of carbon as a coolant in the O^{+2} zone. This suggests that the strong [C I] emission is not due to a high carbon abundance.

We recently attempted to increase the amount of electron collisional excitation of C^0 by increasing the X-ray component of the ionizing spectrum in the models in the fashion of Halpern and Grindlay (1980). However, due to observational constraints on the Crab X-ray continuum, we were unable to enhance the strength of [C I] $\lambda\lambda$9823, 9850 by more than a factor of 2.

Péquignot and Dennefeld (1983), in their model which matched the observed [C I] emission at position M2, assumed a dielectronic recombination rate for $C^+ \rightarrow C^0$ which was roughly 5 times larger than the radiative rate. Recently, Nussbaumer and Storey (1983) calculated the former and found it to be about 3 times *smaller* than the latter for the relevant temperature range. Although experimental work by Mitchell *et al.* (1983) suggests that some calculated rates may be underestimated by a factor of 3 or more, it would appear that dielectronic recombination cannot account completely for the high observed [C I] $\lambda\lambda$9823, 9850 in the Crab.

Collisional excitation by H^0 might play a role in [C I] production in the Crab, since $N(H^0)/N_e \approx 10$ in the C^0 region, as inferred from Henry and MacAlpine (1982). In addition, the gas in this zone is expected to be warm ($T_e \approx 8000$ K) due to heating by a power-law spectrum consisting of EUV and X-ray photons which are absent in stellar continuum heating of H II regions and planetary nebulae. Thus, while H^0 collisional production of [C I] may be insignificant in most H^0

regions because of low T_e ($\lesssim 10^3$ K), conditions in the Crab may make this process important.

Calculations by Smeding and Pottasch (1979) point out the importance of H^0 in collisionally exciting the fine-structure lines of [C I] (see their Fig. 7) under temperatures and density conditions similar to those found in the C^0 zone of the Crab filaments. To assess the contribution made by H^0 to the collisional excitation of [C I] $\lambda\lambda$9823, 9850, we employ equations (42), (47), and (49a) from Bahcall and Wolf (1968) to determine a rate coefficient for the relevant transition $^3P \rightarrow {}^1D$. Although Bahcall and Wolf treated only fine-structure lines, their expressions are probably sufficient for estimating the amount of H^0 excitation of $\lambda\lambda$9823, 9850, to within a factor of 2 or so. Using collision strengths from Péquignot and Aldrovandi (1976), we find that the ratio, Ψ, of collisional excitation by H^0 relative to that by e^- for conditions in the C^0 regions of the filaments is given by

$$\Psi = [(1/f) - 1]2.85 \times 10^{-4} T^{2/3} , \quad (2)$$

where f is the fractional ionization of hydrogen, $N(H^+)/N(H)$. For $\Psi = 1$ (i.e., equal contributions from H^0 and e^-) and a representative temperature of 8000 K, $f = 0.10$. Thus, for values of f and T_e found in the C^0 region, our calculations suggest that the strong [C I] $\lambda\lambda$9823, 9850 emission might be due in part to collisional excitation by H^0. Further investigations using more accurate expressions for rate coefficients are, therefore, of great importance for determining the excitation mechanism(s) responsible for strong [C I] emission in the Crab. In future it would also be important to attempt to observe the [C I] fine-structure lines in the Crab at 370 and 610 microns, since these data could be used to evaluate more completely the role of H^0 in collisional excitation. These lines were recently observed in the Orion nebula by Phillips and Huggins (1981). However, because of much higher temperatures (and therefore broader features) in the Crab than in the H^0 zone of Orion, the expected antenna temperature per unit of resolvable velocity width for the fine-structure lines is too low to be observable with present instrumentation (T. G. Phillips 1982, private communication).

In a number of filaments we observed emission near λ10075. However, since this occurs at the red end of the spectrum where calibration lines are absent, the wavelength solutions are probably inaccurate. The emission is too strong to be P7 λ10049, and we believe it is most likely He II λ10123, whose predicted strength relative to He II λ4686 of 0.26 (see Osterbrock 1974) agrees closely with observed values in most cases, assuming that the reddening is constant across the nebula. We also note that, at positions FK6, FK8, FK9, and HMK4, we observed faint emission at λ8580, which we identify as [Cl II]. This line was observed by Danziger and Aaronson (1974) in the Orion nebula and by Condal (1982) in NGC 2440. However, its faintness in the Crab prevents us from estimating the abundance of Cl^+. The ionization potential of Cl^0 is close to that of H^0, and thus [Cl II] λ8580 most likely originates in the O^+ region. In addition, faint [Ca II] λ7291 is visible in many filaments on the blue wing of the [O II] λ7325 line.

The ratio of [O II] λ7325/λ3727 is sensitive to electron temperature and, to a lesser extent, density. We calculated this line ratio for a range of values of T_e and N_e for a five-level atom. By employing the values for N_e for each position as determined from [S II] measurements by Fesen and Kirshner (1982) and Davidson *et al.* (1982), we derived the [O II] temperatures listed in Table 5 for those positions whose spectra could be linked to optical data through the [S II] doublet. [We actually used values for N_e which were twice as high, since N_e should be higher in the O^+ zone where $N(H^+)/N(H)$ is much greater.] Our temperatures agree reasonably well with those for [N II] and [O II] given by Fesen and Kirshner as well as predicted electron temperatures in the O^+ regions of models for FK5 and FK8 by Henry and MacAlpine.

TABLE 5

[O II] TEMPERATURES

Position	Temperature (K)
FK1	5800 ±2000
FK5	9500 ±2000
FK6	7500 ±3000
FK7	9800 ±1500
FK8	8500 ±2000
FK10	>15000
M2.....	14000 ±3000

Dennefeld and Péquignot (1982) observed several features (labeled *a*, *b*, *c*, and *d* in their Fig. 1) which they attributed to high-velocity gas. We observed lines which correspond to their feature *a* at FK8 as well as M2, although lines similar to their *b*, *c*, and *d* are not evident in either spectrum. (The absence of *c* and *d* in our spectra could be the result of poor sky subtraction). However, feature *a* is quite likely redshifted Hα or [N II] λ6584, associated with gas receding at roughly 1500–2000 km s^{-1}.

[Ni II] λ7378 was first detected in the Crab by Miller (1978), who found it to be comparable in strength to nearby [O II] λ7325. Fesen and Kirshner (1982) observed [Ni II] emission at three locations. The λ7378 line is present at all positions which we observed, and, in some cases, it is stronger than Hβ. The presenece of other [Ni II] lines, particularly λ7411, is not expected, based on the calculations of Nussbaumer and Storey (1982). We have already pointed out that the strengths of [Ni II] and [S II] are highly correlated (see Table 4), so these lines probably originate from the same portion of a filament (i.e., the H^0 zone). Thus, the relative abundance $N(Ni)/N(S)$ can be estimated directly from our data, since, based on ionization potential considerations, $N(Ni)/N(S) \approx N(Ni^+)/N(S^+)$ in this zone. Data for Ni^+ from Nussbaumer and Storey (1982) indicate that, to a good approximation, [Ni II] λ7378 emission results only from collisional excitation of the $^2F_{7/2}$ level from the ground followed by radiative de-excitation. For S^+, however, effects of collisional de-excitation must be considered at densities observed in the filaments. Thus, the ratio $N(Ni)/N(S)$ is determined by the following relation:

$$\frac{N(Ni^+)}{N(S^+)} = \frac{I([Ni\ II])}{I([S\ II])} \cdot \frac{\chi A_{6716} E_{6716} + \chi' A_{6731} E_{6731}}{N_e q(Ni^+)(A_{7378}/A_T) E_{7378}} , \quad (3)$$

where the first term on the right is the ratio of line strengths, while the second term accounts for the collisional excitation and radiative de-excitation rates and energies of the relevant lines. In this case, χ and χ' are the level populations of the

S^+ ion giving rise to λ6716 and λ6731, respectively; A is the transition rate for each line, and E is the associated energy; $q(Ni^+)$ is the collisional excitation rate to the $^2F_{7/2}$ level of Ni^+; and A_T is the total transition rate from the relevant upper level of Ni^+. We employed data from Pradhan (1978) and Mendoza and Zeippen (1982) to determine the level populations of the S^+ ion. For $T_e = 8000$ K and $N_e = 1150$ cm^{-3}, values representative of those observed by Fesen and Kirshner (1982), and our average observed value for $I(\lambda7378/I(\lambda6724)$ of 0.14, we find that $N(Ni)/N(S) = 2.4$. We compare this with the solar ratio of 0.13 (see Allen 1973) and find that Ni may be roughly 18 times more abundant relative to S in the Crab than elsewhere. A similar analysis for $N(Fe)/N(S)$, using our measured strengths of [Fe II] λ8617 and data from Nussbaumer and Storey (1980), yields $N(Fe)/N(S) = 1.4$. In this case, the solar ratio (Allen 1973) is 2.5. Since Henry and MacAlpine (1982) found the relative sulfur abundance to be near or below normal in the Crab, it appears that the abundance of iron may be below normal. In addition, our results imply that $N(Ni)/N(Fe) = 1.7$, or more than 30 times higher than the solar level.

Of course a more accurate determination of the relative abundances of Ni and Fe should account for the presence of some S^{+2} in the Ni^+–Fe^+ zone. However, the individual abundances derived in this fashion would not be expected to differ by more than a factor of 2 from those determined here, while the ratio $N(Ni)/N(Fe)$ should remain virtually unchanged.

In an effort to understand the results for the Ni and Fe abundances in the Crab filaments, similar calculations were performed for the Orion nebula, using relative line strengths from Grandi (1975). Presumably this object contains material which has not been processed nucleosynthetically, and thus offers a test of our abundance determination techniques. We found a solar value for $N(Ni)/N(S)$ but a below-solar value for $N(Fe)/N(S)$. In the latter case, however, our results agreed with previously published iron abundances for Orion. Finally, $N(Ni)/N(Fe)$ was well above the solar value; in fact, the value for Orion was similar to that found for the Crab.

While it is possible that errors in atomic data or neglected physical processes might in part explain these results, we feel it is unlikely that they could account for the order of magnitude enhancement of $N(Ni)/N(Fe)$ derived for both the Crab and Orion. A possible alternative interpretation is that iron possesses a larger affinity for grain formation than does nickel. Thus, in the case of the Crab, the high value for $N(Ni)/N(S)$ may reflect a true enhancement of the iron peak elements, while $N(Fe)/N(S)$ may be low because much of the iron is in the solid state. This interpretation is supported somewhat by the solar value derived for $N(Ni)/N(S)$ coupled with the low value for $N(Fe)/N(S)$ in Orion.

IV. SUMMARY

We have obtained spectra from approximately 6500 Å to 10200 Å for 14 positions among the Crab Nebula filaments. Nine of these locations have been observed previously in the optical region, and the combination of all available data yields the following points:

1. The [Fe II] λ8617 line is roughly one-fourth the strength of Hβ (i.e., stronger than most other lines of Fe) throughout the nebula, making it suitable for deriving an iron abundance.

2. The observed [S III] λ9532/[S II] λ6724 ratio is directly correlated with [O III] λ5007/[O II] λ3727, contrary to the model results of Henry and MacAlpine (1982). This may suggest that a lower pressure actually exists in the filaments than was adopted for the models.

3. The strengths of [Ni II] λ7378 and [S II] λ6724 are directly correlated. [C I] λ9850, on the other hand, is not strongly correlated with either [Ni II] or [S II], even though it presumably is produced in the same region, based on ionization potential considerations.

4. The strength of [C I] λ9850 emission in most of the filaments is at least several times stronger than is predicted by the photoionization models of Henry and MacAlpine (1982). Collisional excitation by H^0, heretofore ignored in all photoionization models of the Crab filaments, may account for part of the [C I] emission.

5. Observed [O II] temperatures agree closely with earlier measurements by Fesen and Kirshner (1982), as well as with results of photoionization models.

6. The relative abundance of Ni may be at least an order of magnitude above cosmic levels, while that of Fe appears to be slightly below normal. The high Ni abundance may actually be reflecting a true enhancement of the iron peak elements, while the low Fe abundance suggests that it is more easily incoporated into grains.

The question of the nickel and iron abundances demands immediate attention, since these abundances are important for deducing the nature of the Crab's progenitor and the physical events which occurred during the supernova event. In addition, if nickel is in fact a more suitable diagnostic for the iron peak element abundances due to a greater affinity of iron for grain formation, it would be important to attempt to observe Ni in other remnants, particularly those of Type I events, in which the abundance of iron is expected to be high.

Equally interesting in its implications is the possibility of collisional enhancement of [C I] emission by H^0. The warm, neutral gas in the Crab filaments seems to provide the conditions under which such excitation could take place. However, this question cannot be further investigated either in the Crab or in other parts of the interstellar medium until more work is done to calculate the necessary collision rate coefficients.

Finally, we note that there are other considerations, not explicitly examined in this paper, which may influence line emission from Crab nebula filaments. Because the age of the filaments is comparable with the time required for gas past the Strömgren distance to recombine, ionization equilibrium calculations may not give a completely accurate description of conditions in the H^0 zones. Also, it is likely that the filaments are subjected to a considerable flux of high-energy particles. Ptak and Stoner (e.g., 1973) have discussed some of the ways in which superthermal particles can influence gas conditions and line emission. Although it is not obvious how these considerations could selectively enhance [Ni II] or [C I] emission, we believe they are worthy of further investigation.

We wish to express our thanks to the director and staff of Kitt Peak National Observatory for their capable assistance during the observing run and with the data reductions. In particular we are grateful to J. Barnes, J. DeVeny, J. Goad, S. Hammond, and P. Schmidtke. We also acknowledge useful

discussions with A. Condal, K. Davidson, R. Fesen, P. Harrington, K. Nomoto, D. Osterbrock, T. Phillips, C. Price, A. Uomoto, G. Williams, and S. Woosley. In addition, we thank G. Williams for providing the plotting routines and Jean Gallagher at JILA for helping to locate information about excitation of neutral carbon. R. B. C. H. is grateful for support received at the University of Michigan from the Clinton B. Ford Fellowship and a Rackham Graduate School thesis grant, as well as computer funds from the University of Michigan and University of Delaware. This research was supported by NSF grants AST-8204215, AST-815050 at Michigan, and AST-8115095 at Delaware.

REFERENCES

Allen, C. W. 1973, *Astrophysical Quantities* (3d ed.; London: Athlone), p. 31.
Aller, L. H., and Liller, W. 1959, *Ap. J.*, **130**, 45.
Bahcall, J. N., and Wolf, R. A. 1968, *Ap. J.*, **152**, 701.
Bass, A. M., and Garvin, D. 1962, *J. Mol. Spectrosc.*, **9**, 114.
Broadfoot, A. L., and Kendall, K. R. 1968, *J. Geophys. Res.*, **73**, 426.
Condal, A. R. 1982, *Astr. Ap.*, **112**, 124.
Condal, A., Fahlman, G., Walker, G., and Glaspey, J. 1981, *Pub. A.S.P.*, **93**, 191.
Dalgarno, A., and Butler, S. E. 1978, *Comments Atom. Mol. Phys.*, **7**, 129.
Danziger, I. J., and Aaronson, M. 1974, *Pub. A.S.P.*, **86**, 208.
Davidson, K. 1978, *Ap. J.*, **220**, 177.
———. 1979, *Ap. J.*, **228**, 179.
Davidson, K. *et al.* 1982, *Ap. J.*, **253**, 696.
Dennefeld, M., and Andrillat, Y. 1981, *Astr. Ap.*, **103**, 44.
Dennefeld, M., and Péquignot, D. 1982, *Astr. Ap.*, preprint.
Dennefeld, M., and Stasińska, G. 1983, *Astr. Ap.*, **118**, 234.
Feldman, F. R. 1979, Ph.D. thesis, University of Michigan.
Fesen, R. A., and Kirshner, R. P. 1982, *Ap. J.*, **258**, 1.
Fesen, R. A., Kirshner, R. P., and Chevalier, R. A. 1978, *Pub. A.S.P.*, **90**, 32.
Foukal, P. 1974, *Pub. A.S.P.*, **86**, 211.
Garstang, R. H. 1968, in *IAU Symposium 34, Planetary Nebulae*, ed. D. E. Osterbrock and C. R. O'Dell (Dordrecht: Reidel), p. 143.
Grandi, S. A. 1975, *Ap. J. (Letters)*, **199**, L43.
Halpern, J. P., and Grindlay, J. E. 1980, *Ap. J.*, **242**, 1041.
Henry, R. B. C., and MacAlpine, G. M. 1982, *Ap. J.*, **258**, 11.
Jewitt, D. C., Kupferman, P. N., Danielson, G. E., and Maran, S. P. 1983, *Ap. J.*, **268**, 683.
MacAlpine, G. M. 1972, *Ap. J.*, **175**, 11.
Mendoza, C., and Zeippen, C. J. 1982, *M.N.R.A.S.*, **198**, 127.
Miller, J. S. 1973, *Ap. J. (Letters)*, **180**, L83.
———. 1978, *Ap. J.*, **220**, 490.
Mitchell, J. B. A., Ng, C. T., Forand, J. L., Levac, D. P., Mitchell, R. E., Sen, A., Miko, D. B., and McGowan, J. W. 1983, *Phys. Rev. Letters*, **50**, 335.
Nussbaumer, H., and Storey, P. J. 1980, *Astr. Ap.*, **89**, 308.
———. 1982, *Astr. Ap.*, **110**, 295.
———. 1983, *Astr. Ap.*, in press.
Osterbrock, D. E. 1974, *Astrophysics of Gaseous Nebulae* (San Francisco: Freeman).
Péquignot, D., and Aldrovandi, S. M. V. 1976, *Astr. Ap.*, **50**, 141.
Péquignot, D., and Dennefeld, M. 1983, *Astr. Ap.*, **120**, 249.
Phillips, M. M. 1978, *Ap. J.*, **226**, 736.
Phillips, T. G., and Huggins, P. J. 1981, *Ap. J.*, **251**, 533.
Pradhan, A. K. 1978, *M.N.R.A.S.*, **184**, 89P.
Ptak, R. L., and Stoner, R. E. 1973, *Ap. J. (Letters)*, **179**, L89.
Smeding, A. G., and Pottasch, S. R. 1979, *Astr. Ap. Suppl.*, **35**, 257.
Woltjer, L. 1958, *Bull. Astr. Inst. Netherlands*, **14**, 39.
Wu, C-C. 1981, *Ap. J.*, **245**, 581.
Wyckoff, S., and Murray, C. A. 1977, *M.N.R.A.S.*, **180**, 717.

RICHARD B. C. HENRY: Department of Physics, Sharp Laboratory, University of Delaware, Newark, DE 19716

ROBERT P. KIRSHNER and GORDON M. MACALPINE: Department of Astronomy, University of Michigan, Ann Arbor, MI 48109